www.elsevier.com/locate/yjtbi

Cell type-dependent, infection-induced, aberrant DNA methylation in gastric cancer

Dimitri Perrin, Heather J. Ruskin, Tohru Niwa

PII: S0022-5193(10)00115-3
DOI: doi:10.1016/j.jtbi.2010.02.040
Reference: YJTBI 5893

To appear in: *Journal of Theoretical Biology*

Received date: 7 October 2009
Revised date: 5 January 2010
Accepted date: 23 February 2010

Cite this article as: Dimitri Perrin, Heather J. Ruskin and Tohru Niwa, Cell type-dependent, infection-induced, aberrant DNA methylation in gastric cancer, *Journal of Theoretical Biology*, doi:10.1016/j.jtbi.2010.02.040

Cell type-dependent, infection-induced, aberrant DNA methylation in gastric cancer

Dimitri Perrin*,[a], Heather J. Ruskin[a], Tohru Niwa[b]

[a] *Centre for Scientific Computing & Complex Systems Modelling, Dublin City University, Ireland*
[b] *Carcinogenesis Division, National Cancer Center, Tokyo, Japan*

Abstract

Epigenetic changes correspond to heritable modifications of the chromatin structure, which do not involve any alteration of the DNA sequence but nonetheless affect gene expression. These mechanisms play an important role in cell differentiation, but aberrant occurrences are also associated with a number of diseases, including cancer and neural development disorders.
In particular, aberrant DNA methylation induced by *H. Pylori* has been found to be a significant risk factor in gastric cancer. To investigate the sensitivity of different genes and cell types to this infection, a computational model of methylation in gastric crypts is developed.
In this article, we review existing results from physical experiments and outline their limitations, before presenting the computational model and investigating the influence of its parameters.

Key words: Cancer, Computational model, DNA methylation, Epigenetics

1. Introduction

Early advances in Genetics led to the *all-genetic* paradigm: the phenotype is a deterministic consequence of the genotype. Obvious counter-examples were outlined and this was later amended: visible characteristics of a living organism (phenotype, P) combine hereditary genetic (genotype, G) and environmental factors (E). This is sometimes summarised as $P = G + E$.

*Corresponding author
Email address: dperrin@computing.dcu.ie (Dimitri Perrin)

However, differences between monozygotic twins can be seen even for high heritability diseases such as schizophrenia, while identification of environmental factors, e.g. smoking and air quality for lung cancer, (Spurny, 1996; Mucha et al., 2006), is relatively rare.

Early work by Waddington (1949), and more recently over the last decade, e.g. Bird (2002); Wilkins (2005), has emphasised that genotype expression can be altered without changing DNA sequence itself, a phenomenon called *Epigenetics*: $P = G + E + EpiG$.

Epigenetic mechanisms involve heritable alterations in *chromatin structure*, (e.g. *DNA methylation* and *histone acetylation*), amongst other epigenetic "signatures". In turn these regulate gene expression, but do not involve changes in DNA sequence. These "stable alterations" arise during proliferation and persist through cell division (Feinberg and Tycko, 2004). While information within the genetic material is not changed, instructions for its assembly and interpretation may be.

Such alterations have, in particular, been linked with tumor-suppressor inactivation and cancer initiation (Esteller, 2007). In this study, we focus on aberrant DNA methylation induced by *H. Pylori* infection. This modification has recently been associated with higher cancer risk. We summarise the results obtained from physical experiments, and propose a computational model to complement these.

2. Infection-induced epigenetic perturbations and cancer initiation

2.1. DNA methylation

DNA methylation corresponds to the addition of a methyl group to a cytosine. In humans, only 1% of DNA bases undergo DNA methylation. In differentiated cells, DNA methylation is typically limited to CpG dinucleotides, while non-CpG methylation can be found in embryonic stem cells, (Dodge et al., 2002).

Of particular interest are *CpG islands*. These correspond to areas with higher proportion of CpG, and are formally defined as follows (Gardiner-Garden and Frommer, 1987):

- Length of the considered region is at least 200 base pairs.
- GC percentage is greater than 50%, (i.e. more than half of amino-acids are cytosine or guanine).

- Observed/expected CpG ratio is greater than 60%.

In humans, these islands are found in or near to 70% of gene promoters, (Saxonov et al., 2006). While most CpG dinucleotides are methylated over the genome, methylation of a CpG island is specifically associated to silencing of the associated gene. Aberrant changes in CpG island methylation are, therefore, linked with abnormal gene expression.

2.2. Infection-induced methylation in gastric cancers

Epigenetic alterations in non-disease tissues can be used as markers for disease risk and past exposure to some disease-inducing factors. In particular, current focus is on detection of aberrant DNA methylation in non-cancerous gastric mucosae, as the presence of such patterns can be used as a marker for both the risk of gastric cancers and for past exposure to *Helicobacter pylori*. A detailed presentation in the context of this study is proposed by Nakajima et al. (2008). For convenience, main points are summarised here.

In cancer development, aberrant DNA methylation is involved at two levels:

- Overall *hypomethylation*, which affects repetitive DNA sequences and causes both chromosomal instability, and, hence, tumours, (Gaudet et al., 2003), as well as aberrant expression of normally methylated genes, (Smet et al., 1999).

- Regional *hypermethylation*, most of which affects CpG islands and causes, (if these islands are located in gene promotion region), transcriptional silencing of the downstream gene. In the context of cancer, methylation affecting tumour suppressor genes is well documented, see e.g. (Jones, 2002; Baylin and Ohm, 2006). This is sometimes referred to as *driver methylation*, because of causal involvement in carcinogenesis, (as opposed to *passenger methylation*, which refers to genes whose methylation is a consequence of cancer development, and therefore requires careful analysis of newly detected genes (Ushijima, 2005)).

In the context of gastric cancers, gene inactivation, (e.g. for tumour suppressor gene p16), is more frequently a consequence of aberrant promoter methylation than of defaults at the genetic level, (Ushijima and Sasako, 2004), but Kaneda et al. (2002) also observed that low levels of aberrant methylation occur in non-cancerous mucosae of cancer patients. This was

tested against tissues from healthy individuals, and it was found that methylation levels for these patients were one to two orders of magnitude higher in *H. pylori*-positive individuals than *H. pylori*-negative individuals (Maekita et al., 2006). This is a very significant finding, since *H. pylori* is known to be a major risk factor for gastric cancers.

It was also highlighted that part of this hypermethylation is *temporary* and will decrease after eradication of infection. This is not due to active demethylation, but simply to cell turnover. The structure of the gastric crypt, (one stem cell, multiple progenitor cells and many differentiated cells, as shown in Figure 1), is the cause for this two-part methylation, where:

- The permanent component is due to methylation of stem cells. Since methylation is conserved during cell division, progenitor and differentiated cells, obtained from an aberrantly methylated stem cell, will exhibit identical abnormal patterns.

- The temporary component is due to methylation in progenitor and differentiated cells. This, if the stem cell of the crypt is not methylated, will disappear because of cell turnover and creation of new, unmethylated, cells.

3. Experimental limitations and computational alternative

3.1. Issues: experimental cost and granularity of the results

Investigation of infection-induced methylation relies on a time-consuming experimental protocol. Based on fixed infection dynamics, several lines of rodents are used: one line is infected for an extended period, (for instance from week 5 to week 55), a second is used as a control, (no infection), while a third is subjected to the eradication procedure only, (at week 55 in the current instance), in case this itself induces aberrant methylation. As the experiment progresses, samples are regularly taken from each population, and the average methylation level is obtained for the genes under investigation. Each sample contains an average of thirty cells, and requires termination of the sampled rodent.

This protocol provides a suitable proxy to investigate aberrant methylation in humans, as the behaviour for cell types of interest is similar, (see e.g. Nakajima et al. (2009); Niwa et al. (2010) for details). Yet, while this experimental protocol provides essential results, (see Nakajima et al. (2008)

for a more comprehensive presentation), there are a number of limitations. These include *reproducibility*: each experiment lasts over a year, and requires large rodent populations. This is an obstacle to more comprehensive studies, for instance involving multiple infection dynamics. Investigating these would be particularly interesting, as the clearance rate then becomes crucial, but this is not immediately feasible, at least not *in vivo*.

The experimental contraints also limit the number of sampling time-points. To satisfy statistical assumptions, each time-point requires multiple samples, taken from each sub-population, which implies a rapid increase, over the extended period, of the overall population required for the experiment. Given this, the sampling intervals is subject to practical limitation: typically every five to ten weeks under "stable" conditions, and every week at most during transitions, (initiation and eradication of the infection).

This, in addition to being able to obtain only the average methylation level, results in low granularity of the results. The "real-time" dynamics of epigenetic changes at the cell level, or even crypt level, are not accessible.

Gaining a better insight into these methylation dynamics, both during infection, (summarised in Figure 2a), and in the long term, (Figure 2b), is the objective of the prototype model we have developed. This is detailed in the following.

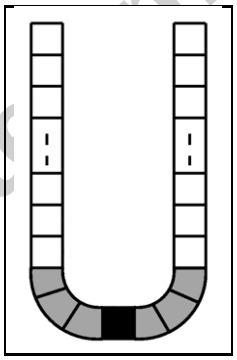

Figure 1: Structure of a gastric crypt, with one stem cell (black), a few progenitor cells (grey), and, approximately, one hundred differentiated cells on each side

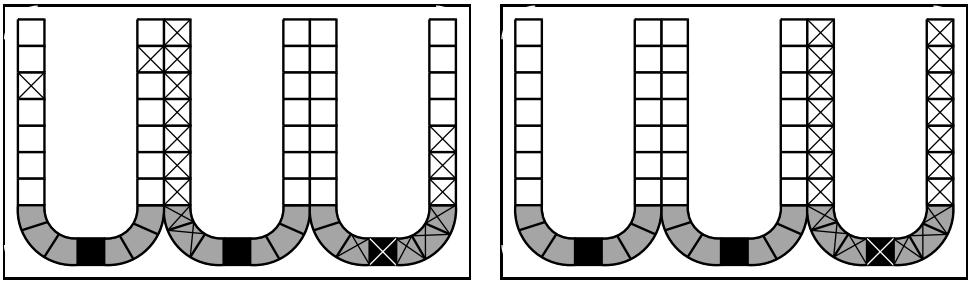

(a) During H. Pylori infection, cells can be methylated, with different probabilities, depending on their type. Methylation status is conserved through cell division, (from stem to progenitor cell, and from progenitor to differentiated cell).

(b) After eradication, only crypts where the stem cell was methylated conserve aberrant methylation, (which is propagated through the whole crypt, during cell divisions).

Figure 2: Methylation dynamics in gastric crypts. Colour represents cell type, (black for stem cells, grey for progenitor cells, white for differentiated cells). Aberrant methylation is shown with a cross inside the cell.

3.2. Computational model

3.2.1. Structure and typical iteration

To investigate the dynamics of infection-induced aberrant methylation in the crypt, we implement an object-oriented model of the entities involved, (samples, crypts, cells). Each entity corresponds to a computing object, and may inherit other objects, (e.g. a crypt contains cells). Each object has a number of attributes which characterise it further, (e.g. each cell has a type: stem cell, progenitor cell, or differentiated cell).

A sample, which mimics *in silico* the samples obtained *in vivo* during the physical experiments described above, is implemented as an array of crypts. Each crypt is initialised with one stem cell, six progenitor cells, and one hundred differentiated cells on each "wall" of the crypt. Initially, no cell is aberrantly methylated.

At each time step, (fixed at one minute for future inclusion of histone modifications), each crypt is updated, as follows. First, cells at the top of both "walls" are analysed and, as these have a finite life span, are removed if necessary. This is followed by update of the bottom of the crypt. A new cell may be created on each side, and progenitor cells may be replaced, (as these are limited in terms of number of differentiated cells produced prior

to replacement by a new progenitor cell). Newly-created cells inherit the epigenetic status of the cell from which they derive through the differentiation process.

Finally, the methylation status of the progenitor and stem cells is updated, depending on cell type and infection status.

The parameters used during this iterative process are described next.

3.2.2. Parameters

Key attributes in control of the cell renewal dynamics in the crypt are the life span of each cell type, and the probability that a new cell is created at the bottom of the crypt. In order to realistically reproduce observed dynamics, the life span, under normal conditions, is 3 days for differentiated cells (i.e. 4320 time steps). When the infection is established, this is reduced to 2.5 days, (3600 time steps). For progenitor cells, the life span is taken to be equivalent to the total number of differentiated cells they can produce, at unit intervals; set at 25 each. Stem cells in the model are considered to have an infinite life span.

To balance the limited life span of differentiated cells, new cells are produced at the bottom of the crypt. At each time step, this occurs with a probability p of 2.3×10^{-3} under normal conditions. This maintains the crypt size to approximately 200 cells. During an infection, this size is increased by a factor ranging from 2 to 4, and this is reflected in the model by increasing p to a value between 7.0×10^{-3} and 1.2×10^{-2}, (randomly chosen for each crypt).

In order to investigate *aberrant methylation*, as described above, probabilities that this change occurs are required, both under normal conditions and during the infection, for both stem cells and progenitor cells. The influence of these parameters is analysed in Section 4.

3.2.3. Transition function

Most model parameters vary depending on the infection status. To account for a progressive transition between the two parameter values, (from normal conditions to established infection), a sigmoid function is used. Equation 1 represents a generic transition between values a and b. In the context of cell production, for instance, a would correspond to $p = 2.3 \times 10^{-3}$, and b to $p = 7.0 \times 10^{-3}$. A typical sigmoid function is shown in Figure 3.

Using this sigmoid function introduces two extra parameters, λ and T, (with $\lambda < 0$ and $T \geq 0$). After eradication of the infection, initial values are

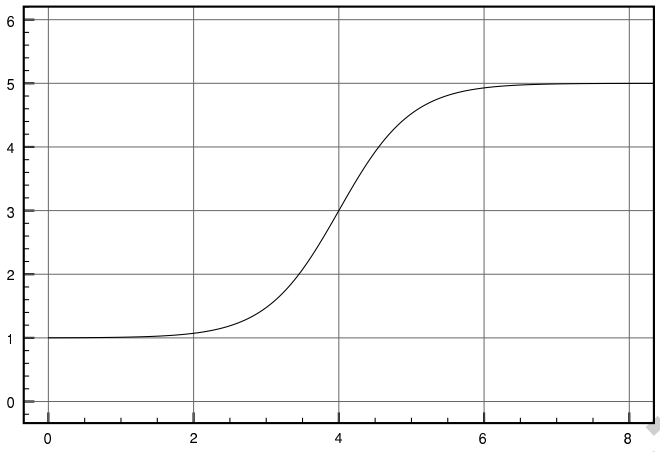

Figure 3: Typical sigmoid function, with $a = 1$, $b = 5$, $\lambda = -2$, and $T = 4$.

restored, (Equation 2). In both equations, units for t are weeks.

$$f(t) = a + (b - a) \times \frac{1}{1 + e^{\lambda(t-T)}} \tag{1}$$

$$f(t) = a + (b - a) \times (1 - \frac{1}{1 + e^{\lambda(t-T)}}) \tag{2}$$

4. Results and discussion

4.1. Reproduction of two-part methylation

The hypothesis, based on physical experimentation, is that, under normal conditions, aberrant stem cell methylation does not occur and that, during *H. Pylori* infection, the probability for methylation of these remains significantly lower than that for progenitor cells.

To validate this, a series of simulations was run, with a range of values for these probabilities, and infection dynamics were set to reproduce experimental conditions: infection, if included, starts at week 5, and is eradicated at week 55.

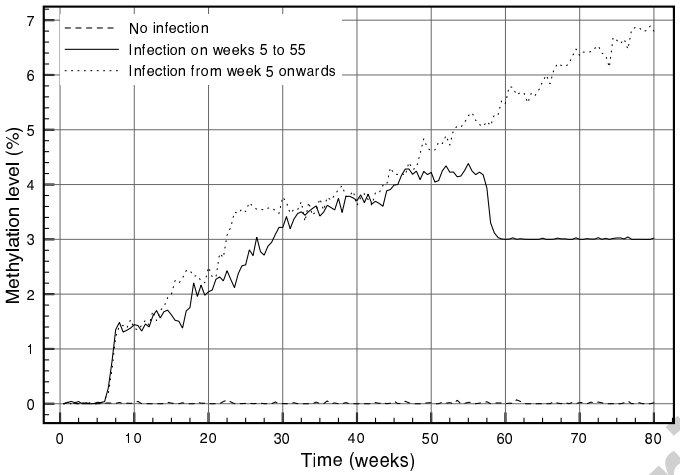

Figure 4: Simulated methylation level. Without infection, methylation is almost absent. *H. Pylori* infection leads to progenitor cell methylation. Unless the stem cell is methylated, this results in rapid but limited fluctuations of the methylation level, since these cells have a finite life span and are routinely replaced with unmethylated cells. The infection also leads, with lower probability, to stem cell methylation, which results in *permanent* and *complete* methylation of the corresponding crypt, (and a correspondingly sharp increase of the methylation level of the sample).

Three typical runs are shown in Figure 4, and correspond to the three populations used during the physical experiments. These results clearly indicate that significant methylation levels can only be obtained through infection and that, after eradication, only part of this aberrant methylation remains. This permanent level is equal to the proportion of methylated stem cells in the sample.

The results from the physical experiments have been successfully reproduced, and the model hypothesis validated. The remainder of this section analyses the sensitivity of this model to its various parameters, and the implications of this sensitivity with respect to the observed phenomena. Because aberrant methylation is modelled as a stochastic process, this analysis is based on multiple simulations for each model configuration. In order to obtain statistically significant values, averages are calculated over twenty sim-

ulations. A similar protocol is used during the *in vivo* experiments, in that several rodents are used to obtain values for each time and each configuration.

4.2. Impact of cell-type dependency

The model is based on specific cell types having different sensitivity to *H. Pylori* infection. In particular, the main conclusion of the physical experiments is that infection-induced aberrant methylation is significantly more likely to occur on progenitor cells than on stem cells, and has a relatively short lifetime.

To account for this, four parameters are necessary. α and β represent the probability of aberrant methylation once the infection is established, for stem cells and progenitor cells respectively. Under normal conditions, the respective probabilities are denoted α_0 and β_0. A first assumption, as mentioned, is that $\alpha \ll \beta$. Based on the experimental information, we can also assume that $\alpha_0 = 0$.

Sensitivity to α is shown in Figure 5. This probability of stem cell methylation at each time step has two consequence for model behaviour: higher values of α increase both (i) the methylation level, at any given point during the infection, and (ii) the level of permanent methylation after eradication. In physical experiments, the level of permanent methylation for various genes was observed to be between 0.04 and 1.02%. This corresponds, in our model, to α between 0 and 0.9×10^{-8}.

Sensitivity to β is shown in Figure 6. Increasing the probability of methylation for progenitor cells only affects the methylation level at a given time-point during the infection. This is increased, but both the rate of increase during infection and the methylation level after eradication are unchanged.

These results are significant, as they imply that accurate values for α and β for any gene can be extracted from the model. Using data from physical experiments, we initially obtain α, by focusing on the level of permanent methylation after eradication of the infection. Then, once α is fixed, the methylation level at several time-points during the infection can be used to deduce β. Finally, variations about the average values both before and after the infection are sufficient to estimate β_0.

4.3. Impact of infection dynamics

4.3.1. Sensitivity to transition periods

Neither the initial size of the crypt nor the size it reaches once the infection is established have any impact on the observed methylation level. This is

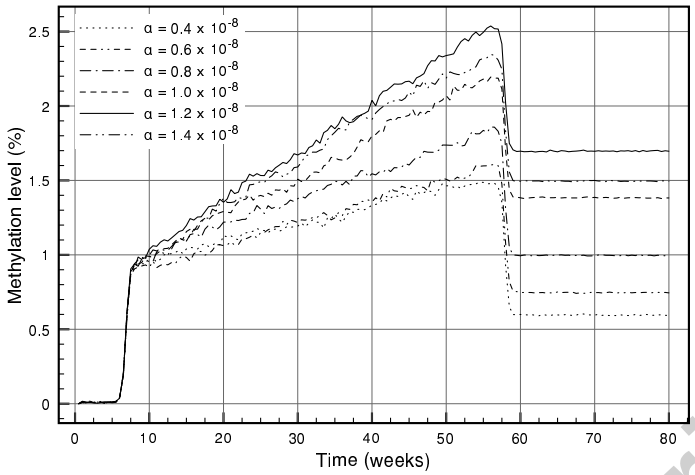

Figure 5: Sensitivity to α. Each curve corresponds to the average methylation level over 20 simulations, for a specific value of α, (probability of stem cell methylation at each time step).

a consequence of the methylation level being a proportion of methylation cells rather the number of such cells, (and has been verified experimentally). However, the transition between these two values does have a significant impact, which we investigate in detail.

Two parameters are used in the sigmoid functions which describe this transition: λ and T. Two sets of values are used during each simulation: λ_s and T_s, (for changes with respect to cell renewal dynamics in the crypt); λ_g and T_g, (for modifications of the methylation probabilities). Figures 4 to 6 were shown for $\lambda_c = \lambda_g = -4$, and $T_c = T_g = 2$. Here, we analyse the impact of these values on the model behaviour.

Figure 7 summarises the effect of reducing λ_g compared to λ_s, (which must coincide with an increase of T_g, so that the transition function remains realistic). This corresponds to a situation where the impact of the infection on aberrant methylation of a specific gene is established more slowly than the effect on crypt size, (through perturbed cell renewal dynamics). In such a case, the average methylation level over the sample is slower to rise, but the most significant difference occurs when the infection is eradicated. Cells are still likely to be methylated, since this transition is slower, but the

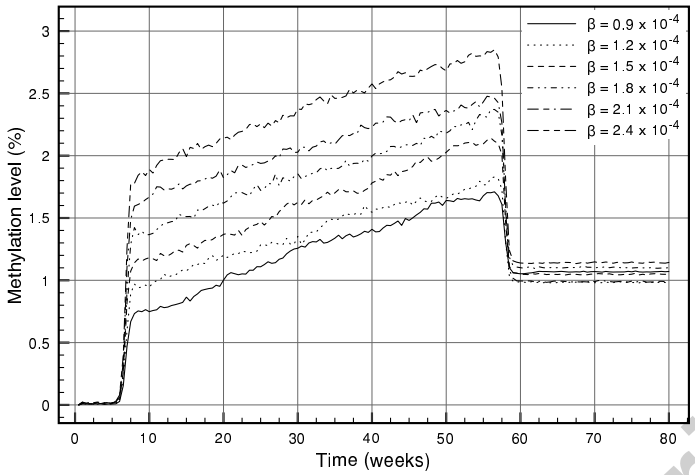

Figure 6: Sensitivity to β. Each curve corresponds to the average methylation level over 20 simulations, for a specific value of β, (probability of progenitor cell methylation at each time step).

crypt size is already decreasing. This results in a brief but sharp increase of the methylation level, as most destroyed cells are unmethylated, (due to low methylation level overall). Such an increase was observed for several genes during the physical experiments, and a difference between λ_s and λ_g is one plausible explanation of this phenomenon. As the observed increase is generally slow, this would correspond to a small difference between the two values.

Figure 8 summarises the effect of reducing λ_s, (which, similarly to before, must coincide with an increase in T_s, so as to maintain realism of the transition function). This occurs when aberrant methylation starts before the crypt size has reached its maximum infected level. The effect is, therefore, opposite to that of reducing λ_s, and a temporary, sharp increase of the overall methylation level is observed when the *H. Pylori* infection begins.

Due to experimental limitations, it was possible to test *in vivo* only one infection configuration, (starting at week 5, and eradicated at week 55). However, shorter infections are not only possible, but can also occur *repeatedly*. These conditions give rise to another series of simulations.

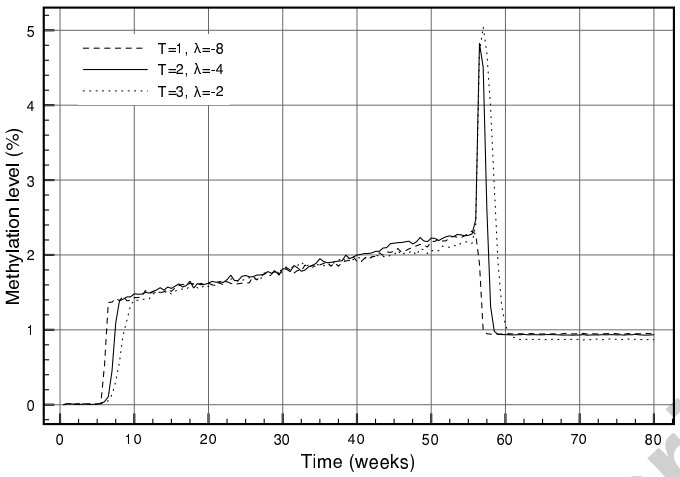

Figure 7: Sensitivity to λ_g and T_g. Each curve corresponds to the average methylation level over 20 simulations, for specific values of λ_g and T_g.

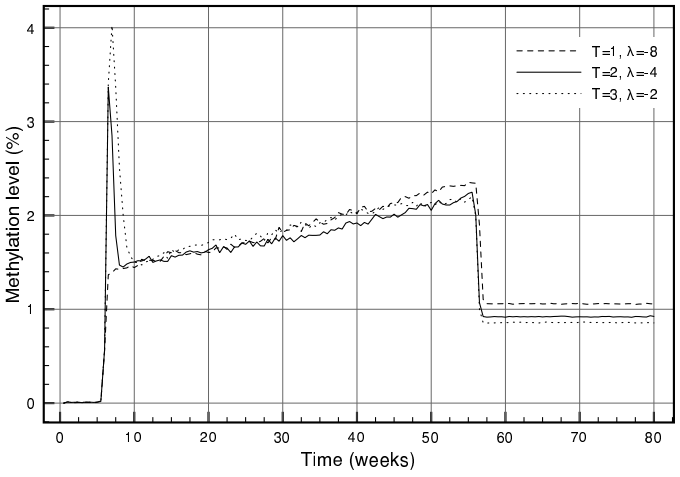

Figure 8: Sensitivity to λ_s and T_s. Each curve corresponds to the average methylation level over 20 simulations, for specific values of λ_s and T_s.

4.3.2. Sensitivity to repeated infections

We first considered two infections, from weeks 5 to 25 and 35 to 55. Figure 9 summarises the results, for $\lambda_g < \lambda_s$, $\lambda_g = \lambda_s$, and $\lambda_g > \lambda_s$. We then simulated a succession of shorter infections, from weeks 5 to 13, 21 to 29, 37 to 45, and 53 to 61, (summarised in Figure 10 for similar configurations of the transition period). As expected from the earlier results, configurations where there is a significant difference between λ_g and λ_g create distortions of the methylation level during transition periods. However, if each occurrence of the infection is long enough, and if there is a sufficient time between these, the parameters related to the transition period have *no impact on the long-term methylation level*. This is of the same order as that for a single infection for which the length would be equal to the combined length of these shorter occurrences.

A significant observation, for short infections, is that the distortions created by differences between λ_g and λ_g may persist for most of the infection period. During physical experiments, (which have to yet to be performed for infection dynamics such as these), this would lead to a significant *over-estimation* of the size of actual changes in methylation.

For clarity, it must be noted that, in Figures 9 and 10, the difference between the long-term methylation level of the three configurations is not a consequence of the values for λ_g and λ_s. In Figure 9, the lower methylation level for the first configuration is a consequence of the methylation of fewer stem cells during the first infection phase for some simulations. In Figure 10, a similar slight underestimation exists, and is a result of fewer methylations during the third infection phase. These differences occurred after the infection was fully established, and are an artefact of the finite number of simulations: the shorter the infection length, the greater the standard variation in the number of methylated stem cells between simulations, (because of very low probability, at each time step, to methylate a stem cell).

A similar increase in the variation can be expected for *in vivo* experiments. Given the limited number of samples at each time-point, this would further reduce the reliability of the measurements under these infection dynamics.

Increasing the number of simulations permits the reduction of this effect in the computational model, but is not a realistic for the *in vivo* counterpart, because of cost and space constraints associated with increasing the rodent population.

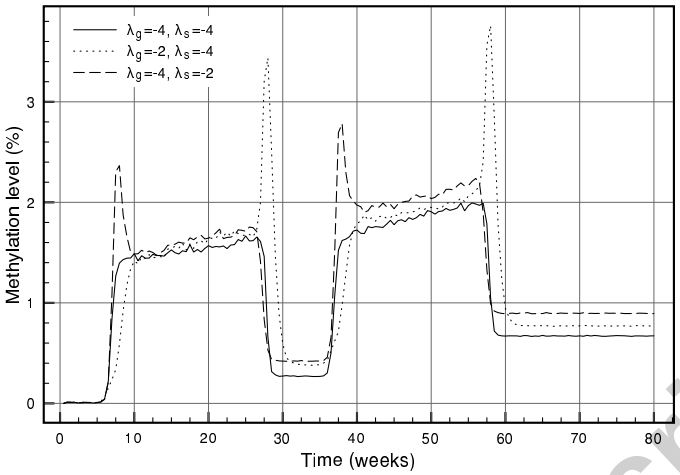

Figure 9: Sensitivity to λ_g and λ_s during repeated 20-week infections.

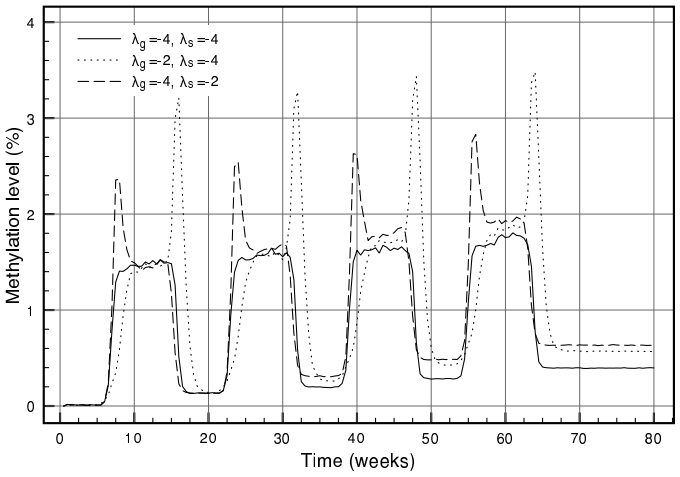

Figure 10: Sensitivity to λ_g and λ_s during repeated 8-week infections.

4.4. Applications

From a single series of physical experiments, it is possible, with the computational model proposed, to extract parameters controlling the aberrant methylation of the genes under consideration. Using these parameters, we can estimate the level of aberrant methylation resulting from any infection pattern, without requiring a biological cell or a sample from the individual, for all genes investigated during the *in vivo* experiments. Further development of the model will focus on other genes of potential interest.

These results offer crucial insights towards a better understanding of the initiation of gastric cancers: methylation levels have been observed to be significantly higher in cases of gastric cancer compared to healthy volunteers (Maekita et al., 2006), and significantly higher in patients with multiple gastric cancers compared to those with a single gastric cancer (Nakajima et al., 2006).

The ability to model such features represents an important milestone in establishing DNA methylation as a marker for gastric cancer risk. This is likely to be generalised to other types of cancer and tissues: aberrant DNA methylation in non-cancerous tissues was also identified e.g. in the colon, (Issa et al., 1994), the liver, (Kondo et al., 2000), and the stomach, (Waki et al., 2002).

A limitation of current *in vivo* and *in vitro* studies is that, while successful in investigating specific phenomena, such experiments so far fail to explain system-wide complex interactions. These may reflect overall system complexity, but technical constraints lead most research groups to focus on a single epigenetic change in a given context. The need for integration of these partial results is crucial to understanding the overall biological system, and computer-based modelling can provide a useful complementary framework in this, as in other fields, (Dove, 2006).

5. Conclusion

The model, developed here, is able to reproduce and complement *in vivo* experiments on cell type-dependent aberrant DNA methylation during *H. Pylori* infection. As such, it provides useful insights on the dynamics of infection-induced aberrant epigenetic changes, which have been linked to gastric cancer initiation.

Costly and time-consuming lab-testing is intrinsic to *in vivo* epigenetic research. This computer-based study demonstrates that *in silico* modelling

can facilitate quantitative methylation analysis and the investigation of key factors influencing disease initiation. The model can thus play a significant role in developing better understanding of gastric cancers. Notably, as an important milestone in establishing DNA methylation as a marker for gastric cancer risk, it contributes to a better identification of at-risk patients.

Furthermore, as the first to successfully reproduce epigenetic events *in silico*, the current version can be seen as a *proof of concept* for more advanced models, incorporating several epigenetic changes and the complex interactions between them. In particular, future model versions will take partial methylation levels into account, and will include histone modifications.

Acknowledgements

The authors would like to thank Prof. Toshikazu Ushijima and his team at the National Cancer Center (Tokyo, Japan), for providing access to their results and participating in a number of thought-provoking discussions on Epigenetics.

Financial support from Science Foundation Ireland (Research Frontiers Programme 07/RFP/CMSR724) is warmly acknowledged.

The authors also wish to acknowledge the SFI/HEA Irish Centre for High-End Computing (ICHEC) for the provision of computational facilities and support.

References

Baylin, S. B., Ohm, J. E., 2006. Epigenetic gene silencing in cancer – a mechanism for early oncogenic pathway addiction? Nature Reviews Cancer 6, 107–116.

Bird, A., 2002. DNA methylation patterns and epigenetic memory. Genes & Development 16, 6–21.

Dodge, J. E., Ramsahoye, B. H., Wo, Z. G., Okano, M., Li, E., 2002. De novo methylation of MMLV provirus in embryonic stem cells: CpG versus non-CpG methylation. Gene 289 (1–2), 41–48.

Dove, A., 2006. Virtual models best live cells at predicting biology. Nature Medicine 12, 1225.

Esteller, M., 2007. Cancer epigenomics: DNA methylomes and histone-modification maps. Nature Reviews Genetics 8 (4), 286–298.

Feinberg, A. P., Tycko, B., 2004. The history of cancer epigenetics. Nature Reviews Cancer 4 (2), 143–153.

Gardiner-Garden, M., Frommer, M., 1987. CpG islands in vertebrate genomes. Journal of Molecular Biology 196 (2), 261–282.

Gaudet, F., Hodgson, J. G., Eden, A., Jackson-Grusby, L., Dausman, J., Gray, J. W., Leonhardt, H., Jaenisch, R., 2003. Induction of tumors in mice by genomic hypomethylation. Science 300, 489–492.

Issa, J.-P. J., Ottaviano, Y. L., Celano, P., Hamilton, S. R., Davidson, N. E., Baylin, S. B., 1994. Methylation of the oestrogen receptor CpG island links ageing and neoplasia in human colon. Nature Genetics 7, 536–540.

Jones, P. A., 2002. DNA methylation and cancer. Oncogene 21, 5358–5360.

Kaneda, A., Kaminishi, M., Yanagihara, K., Sugimura, T., Ushijima, T., 2002. Identication of silencing of nine genes in human gastric cancers. Cancer Research 62, 6645–6650.

Kondo, Y., Kanai, Y., Sakamoto, M., Mizokami, M., Ueda, R., Hirohashi, S., 2000. Genetic instability and aberrant DNA methylation in chronic hepatitis and cirrhosis – A comprehensive study of loss of heterozygosity and microsatellite instability at 39 loci and DNA hypermethylation on 8 CpG islands in microdissected specimens from patients with hepatocellular carcinoma. Hepatology 32, 970–979.

Maekita, T., Nakazawa, K., Mihara, M., Nakajima, T., Yanaoka, K., Iguchi, M., Arii, K., Kaneda, A., Tsukamoto, T., Tatematsu, M., Tamura, G., Saito, D., Sugimura, T., Ichinose, M., Ushijima, T., 2006. High levels of aberrant DNA methylation in Helicobacter pylori-infected gastric mucosae and its possible association with gastric cancer risk. Clinical Cancer Research 12, 989–995.

Mucha, L., Stephenson, J., Morandi, N., Dirani, R., 2006. Meta-analysis of disease risk associated with smoking, by gender and intensity of smoking. Gender Medicine 3 (4), 279–291.

Nakajima, T., Enomoto, S., Ushijima, T., 2008. DNA methylation: a marker for carcinogen exposure and cancer risk. Environmental Health and Preventive Medicine 13 (1), 8–15.

Nakajima, T., Enomoto, S., Yamashita, S., et al., 2009. Persistence of a component of DNA methylation in gastric mucosae after helicobacter pylori eradication. Journal of Gastroenterology Oct. 10 [Epub ahead of print].

Nakajima, T., Maekita, T., Oda, I., Gotoda, T., Yamamoto, S., Umemura, S., Ichinose, M., Sugimura, T., Ushijima, T., Saito, D., 2006. Higher methylation levels in gastric mucosae significantly correlate with higher risk of gastric cancers. Cancer Epidemiology Biomarkers & Prevention 15, 2317–2321.

Niwa, T., Tsukamoto, T., Toyoda, T., et al., 2010. Causal role of helicobacter pylori infection in induction of aberrant DNA methylation in gastric epithelial cells, and critical involvement of inflammation. Cancer Research (in press).

Saxonov, S., Berg, P., Brutlag, D. L., 2006. A genome-wide analysis of CpG dinucleotides in the human genome distinguishes two distinct classes of promoters. Proceedings of the National Academy of Sciences USA 103 (5), 1412–1417.

Smet, C. D., Lurquin, C., Lethe, B., Martelange, V., Boon, T., 1999. DNA methylation is the primary silencing mechanism for a set of germ line- and tumor-specific genes with a CpG-rich promoter. Molecular and Cellular Biology 19, 7327–7335.

Spurny, K. R., 1996. Chemical mixtures in atmospheric aerosols and their correlation to lung diseases and lung cancer occurence in the general population. Toxicology Letters 88, 271–277.

Ushijima, T., Sasako, M., 2004. Focus on gastric cancer. Cancer Cell 5, 121–125.

Ushijima, T., 2005. Detection and interpretation of altered methylation patterns in cancer cells. Nature Reviews Cancer 5, 223–231.

Waddington, C. H., 1949. The genetic control of development. Symposia of the Society for Experimental Biology 2, 145–154.

Waki, T., Tamura, G., Tsuchiya, T., Sato, K., Nishizuka, S., Motoyama, T., 2002. Promoter methylation status of E-cadherin, hMLH1, and p16 genes in nonneoplastic gastric epithelia. American Journal of Pathology 161, 399–403.

Wilkins, J. F., 2005. Genomic imprinting and methylation: epigenetic canalization and conflict. Trends in Genetics 21, 356–365.